Direct observation of electrogenic NH_4^+ transport in ammonium transport (Amt) proteins

Tobias Wacker[a], Juan J. Garcia-Celma[b,c], Philipp Lewe[a], and Susana L. A. Andrade[a,d,1]

[a]Institute for Biochemistry, Albert-Ludwigs University Freiburg, 79104 Freiburg, Germany; [b]Department of Biochemistry, University of Zürich, 8057 Zürich, Switzerland; [c]Institute of Complex Systems–Cellular Biophysics Research Center Jülich, 52428 Jülich, Germany; and [d]BIOSS Centre for Biological Signalling Studies, 79104 Freiburg, Germany

Edited by H. Ronald Kaback, University of California, Los Angeles, CA, and approved June 4, 2014 (received for review April 8, 2014)

Ammonium transport (Amt) proteins form a ubiquitous family of integral membrane proteins that specifically shuttle ammonium across membranes. In prokaryotes, archaea, and plants, Amts are used as environmental NH_4^+ scavengers for uptake and assimilation of nitrogen. In the eukaryotic homologs, the Rhesus proteins, NH_4^+/NH_3 transport is used instead in acid–base and pH homeostasis in kidney or NH_4^+/NH_3 (and eventually CO_2) detoxification in erythrocytes. Crystal structures and variant proteins are available, but the inherent challenges associated with the unambiguous identification of substrate and monitoring of transport events severely inhibit further progress in the field. Here we report a reliable in vitro assay that allows us to quantify the electrogenic capacity of Amt proteins. Using solid-supported membrane (SSM)-based electrophysiology, we have investigated the three Amt orthologs from the euryarchaeon *Archaeoglobus fulgidus*. *Af*-Amt1 and *Af*-Amt3 are electrogenic and transport the ammonium and methylammonium cation with high specificity. Transport is pH-dependent, with a steep decline at pH values of ∼5.0. Despite significant sequence homologies, functional differences between the three proteins became apparent. SSM electrophysiology provides a long-sought-after functional assay for the ubiquitous ammonium transporters.

ammonium transport proteins | Amt/Rh family | cation transport

Ammonium transport (Amt) proteins are a class of trimeric, integral membrane proteins found throughout all domains of life. Despite moderate primary sequence homologies, distinct family members from bacteria, archaea, and eukarya (including humans) share conserved structural features and a high number of conserved amino acid residues that are considered functionally relevant (1–4). Although the involvement of all Amt proteins in transporting NH_4^+/NH_3 across biological membranes is undisputed, their functional context is diverse. Prokaryotes and plants use Amt proteins to scavenge NH_4^+/NH_3—a preferred nitrogen source for cell growth—from their environment, whereas mammals use Amt orthologs, the Rhesus proteins, for detoxification and ion homeostasis in erythrocytes and in the kidney and liver tissues (1, 5, 6).

Three decades ago, Kleiner and coworkers suggested that Amt proteins are secondary active and electrogenic transporters for ammonium (7–9). Various groups have subsequently confirmed this finding by two-electrode voltage-clamp experiments with protein produced recombinantly from RNA injected into *Xenopus laevis* oocytes. Here, plant Amt and Rhesus proteins were the main object of study, but some mechanistic details remained unclear, in particular the distinction between electrogenic NH_4^+ uniport (10–13), NH_3/H^+ symport (11, 12), or electroneutral NH_4^+/H^+ antiport (14, 15). In contrast, bacterial Amt proteins were described as passive channels for the uncharged gas ammonia (NH_3) (16). The first crystal structure for an Amt family member, AmtB from *Escherichia coli* (17), was interpreted to support this hypothesis, and an ongoing controversy concerning the transported species has persisted in the field ever since. Several points have been raised to challenge the possibility of gas channeling, the most critical of which seems to be that at physiological pH the protonation equilibrium of NH_3—with a pK_a of 9.4—would be >99% on the side of charged NH_4^+. This point implies that the import of neutral ammonia gas must be preceded by extracellular deprotonation and followed immediately by intracellular protonation. In summary, the import of NH_3 would thus result in a net NH_4^+/H^+ antiport. Such a mechanism would be electroneutral, but it would be secondary active in the presence of a proton motive force, resulting in a vectorial pumping of ammonium out of the cell—which is, of course, physiologically unreasonable. A second point is that biological membranes are themselves highly permeable for uncharged ammonia, with a permeability coefficient, $P_d = 10^{-3}$ cm·s^{-1}, similar to that of water (18), such that a dedicated transport protein would hardly be required. Westerhoff and coworkers have argued that active Amt transport thus is imperative and that cells must be able to quickly block Amt transport upon intracellular accumulation of ammonium to avoid uncoupling of the proton gradient through back-diffusion of NH_3 (19). In prokaryotes and some plants, this blocking is the task of regulatory GlnK proteins belonging to the signal transducing P_{II} family that bind to corresponding ammonium transporters when their regulatory ligand 2-oxoglutarate, the primary metabolic acceptor for NH_4^+ during nitrogen assimilation, is depleted (20).

The high expectations to understand the mechanism of Amt transport from 3D structures have not been met to date. The available structures of *E. coli* AmtB (17, 21) and its complex with GlnK (22, 23) of *A. fulgidus* Amt-1 (24), *Nitrosomonas europaea* Rh50 (25, 26), and human RhCG (27) all show the same, inward-facing state of the protein. Such apparent structural rigidity would match the picture of a fast channel, whereas active transport is generally considered to involve conformational changes that expose a binding site for the cargo molecule(s) alternatingly

Significance

We have detected and analyzed electrogenic transport of ammonium and methylammonium by members of the ammonium transport (Amt) family of membrane proteins using solid-supported membrane electrophysiology. Amt transport is pH-dependent and occurs at a rate of 30–300 ions per s per trimer, well in the range of other transport proteins. The study establishes, to our knowledge, the first in vitro assay system for Amt transport in a fully controlled setup and settles debate about whether Amt proteins function as passive ammonia channels or active ammonium transporters.

Author contributions: T.W., J.J.G.-C., and S.L.A.A. designed research; T.W. and P.L. performed research; J.J.G.-C. contributed new reagents/analytic tools; T.W., J.J.G.-C., and S.L.A.A. analyzed data; and T.W., J.J.G.-C., and S.L.A.A. wrote the paper.

The authors declare no conflict of interest.

This article is a PNAS Direct Submission.

[1]To whom correspondence should be addressed. E-mail: andrade@bio.chemie.uni-freiburg.de.

This article contains supporting information online at www.pnas.org/lookup/suppl/doi:10.1073/pnas.1406409111/-/DCSupplemental.

to either side of the membrane (28). In addition, the difficulties to detect NH_4^+/NH_3 and to assay Amt transport led to a lack of functional studies carried out in vitro on well-defined systems. An uptake assay with AmtB reconstituted in proteoliposomes was described to provide evidence for passive gas channeling (17), but the methodology was later contested (2). Assays based on the detection of radioactive methylammonium (MA) uptake were only carried out in whole cells of *E. coli*, and studies with voltage-clamp electrophysiology using Amt-1 reconstituted in planar lipid bilayers did not yield conclusive results (our work). A series of potentially important variants have been produced (29–39), but the lack of an adequate functional assay has precluded definite conclusions.

The debate concerning the transport mechanism of Amt proteins has not been settled to date, necessitating a reliable functional in vitro assay. The finding that electrogenic transport was observed in *X. laevis* oocytes, but not in the far smaller membrane patch of a planar lipid bilayer setup, suggested that the transport rate of Amt proteins was possibly too low to lead to a detectable current response, unless a larger number of protein units were incorporated into the bilayer. We have therefore focused on a controlled method of in vitro electrophysiology that allows the simultaneous activation of $>10^8$ protein units, the solid-supported membrane (SSM) electrophysiology (40). With this approach, pioneered by Fendler and coworkers, we were able to detect robust ion currents from isolated and reconstituted Amt proteins.

Results

***Af*-Amt1 Is an Electrogenic Transporter.** To record the electrogenic activity of *Af*-Amt1, liposomes reconstituted with isolated protein were prepared by rapid dilution at a lipid-to-protein ratio (LPR) of 5:1. The proteoliposomes were adsorbed to the phosphatidylcholine monolayer of a hybrid bilayer covering a gold electrode, the SSM (40–42). The resulting, capacitatively coupled system of immobilized vesicles is termed the sensor, and its mechanical stability is such that solutions can swiftly be perfused through the cuvette without loss of electric signal.

To study the electrogenic response of *Af*-Amt1, ammonium concentration jumps were applied to drive transport of the cation into the vesicles. Electrogenic ammonium transport should consequently build up an inside-positive membrane potential, leading to a decrease of the initial driving force and deceleration of the transport rate. This process results in the decay of the measured current toward baseline in a negative feedback loop, such that SSM-based electrophysiology currents are transient (40). When using proteoliposomes reconstituted with *A. fulgidus* Amt-1, the application of 300 mM ammonium concentration jumps at pH 7.0 led to transient currents corresponding to a positive charge displacement (Fig. 1*B*). Two distinct phases were recognized in such transients. First, the ammonium concentration jump triggered a rapid increase of current from the baseline to reach a peak current. Subsequently, the current fell back to baseline, but with a significantly slower rate. The decay time is quantified by the time between the peak current and a half-maximal current intensity ($\tau_{1/2}$). Under our experimental conditions (LPR 5:1, 300 mM NH_4Cl, pH 7.0), we obtained $\tau_{1/2} = 14 \pm 2$ ms, reflecting the establishment of an inside-positive potential due to the electrogenic transport of ammonium. The amplitudes of the transient currents are primarily dependent on the amount of vesicles immobilized on the sensor. From a minimum of 10 distinct sensors prepared from various batches of isolated *Af*-Amt1 and various reconstitutions using a LPR of 5:1, the average observed peak current was 2.2 ± 0.8 nA.

Protein-free liposomes were used as control and for quantification of background currents. Such currents have been described in the literature and are thought to originate from the specific interaction of the ions with the lipid head groups (43).

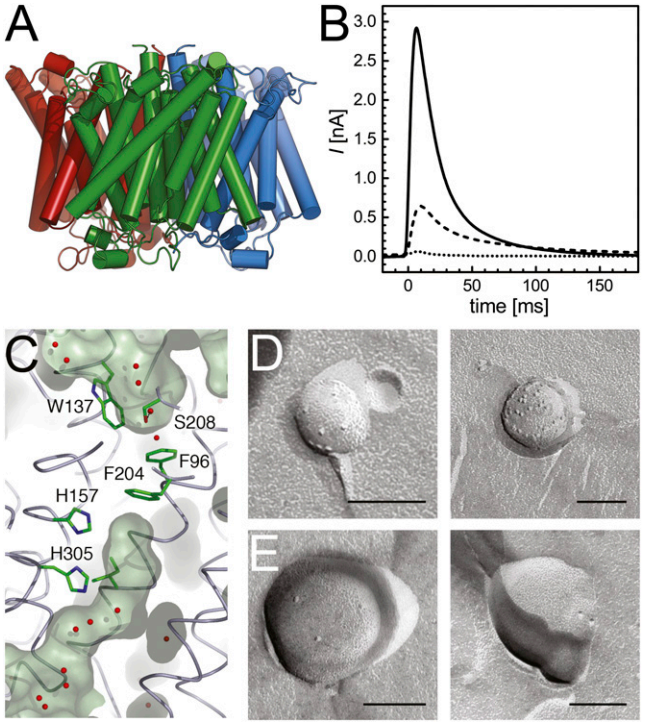

Fig. 1. The ammonium transporter Amt1 from *A. fulgidus*. (*A*) Shown are 3D structure of *Af*-Amt1. The protein forms stable trimers in the membrane, with distinct transport channels in each monomer [Protein Data Bank (PDB) ID code 2B2F]. (*B*) Transient currents recorded from proteoliposomes of *Af*-Amt1 immobilized on a SSM. Although background currents are negligible (dotted), significant transients are obtained with a LPR of 50:1 (dashed) and 5:1 (solid). (*C*) The transport channel commences with a recruitment site that selects for cationic species (W137) that are able to act as hydrogen-bond donors (S208). A transport pathway is sealed off by F96 and F204, indicating that conformational changes are required, a hallmark of transport proteins (PDB ID code 2B2F). (*D* and *E*) Freeze-fracture electron micrographs of proteoliposomes containing *Af*-Amt1 at a LPR of 5:1 (*D*) and 50:1 (*E*). (Scale bars: 100 nm.)

Ammonium background currents amounted to <10% of those recorded with proteoliposomes containing pure *Af*-Amt1 (Figs. 1*B* and 2).

Binding of charged substrates or the occurrence of conformational changes in the immobilized protein might also generate transient currents. Such electrogenic partial reactions (or incomplete transport cycles) have been observed with several secondary active transporters, such as melibiose permease (44) or lactose permease (LacY) (45, 46). To discriminate between both electrogenic responses, the effect of the LPR on the decay time of the transients was investigated. If the observed currents indeed reflected transport of ammonium into the vesicles, the decay time should be proportional to the amount of protein incorporated into each vesicle. Consequently, higher LPR (lower protein density) should result in a longer decay time $\tau_{1/2}$ and vice versa. If, however, the major contribution to the detected currents is an electrogenic partial reaction, the decay time should not be affected by the LPR of the vesicles. *Af*-Amt1 was reconstituted at different LPR and freeze-fracture-etch transmission electron microscopy was used to count molecules within multiple vesicle membranes (Fig. 1 *D* and *E*). At an LPR of 5:1, the density of Amt trimers was 402 ± 57 μm^{-2}, whereas for an LPR of 50:1, the number dropped to 76 ± 15 μm^{-2}. In parallel, the decay time $\tau_{1/2}$ increased from 14 ± 2 ms (LPR 5:1) to 25 ± 3 ms (LPR 50:1) (Fig. 1*B*). The measured transient currents thus indeed reflect electrogenic transport of ammonium into the

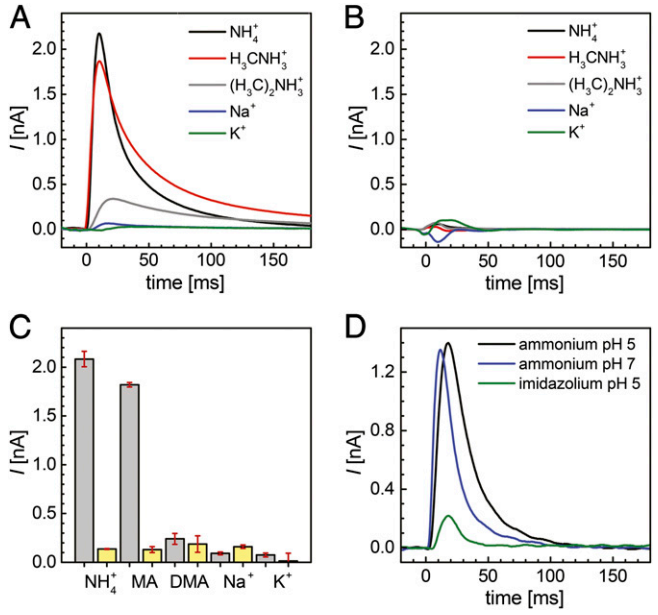

Fig. 2. Substrate specificity of electrogenic transport in *Af*-Amt1. (*A*) Transient currents observed on the same sensor for ammonium (black), MA (red), DMA (gray), and the nonconducting ions sodium (blue) and potassium (green). (*B*) Background currents for all species in *A* were recorded on protein-free liposomes and were found to be negligible. (*C*) Bar graph of the peak currents for the conducted species (gray) and the respective background (yellow). *Af*-Amt1 shows distinct specificity for ammonium and MA. (*D*) Transients for 300 mM NH_4^+ in the active solution at pH 7 (blue) and pH 5 (black) show a slight shift of the peak current, whereas a control (300 mM imidazolium, pH 5.0; green) is not conducted.

vesicles. Moreover, because no significant membrane potential has yet built up when the currents reach their maximum, the measured peak currents reflect the turnover rate of *Af*-Amt1 at zero voltage.

The orientation of Amt trimers in the vesicles was investigated by generating a variant with a C-terminal cleavage site for tobacco etch virus (TEV) protease, *Af*-Amt1^{TEV}. Proteoliposomes containing *Af*-Amt1^{TEV} were subjected to protease digestion and subsequently analyzed by SDS/PAGE (*SI Appendix*, Fig. S1). The digest of the protein was found to be complete, indicating that all molecules inserted into the liposomes in an identical orientation, with outward-facing C termini. Taking this into consideration, we can assign the recorded transient currents to the translocation of 30–300 NH_4^+ per s per $^-$trimer, from the outer solution into the lumen of the vesicles without application of an external voltage.

***Af*-Amt1 Is Selective for Ammonium and MA.** MA ($H_3CNH_3^+$; pK_a = 10.64) is a well-known alternative transport substrate for Amt proteins (7–9, 47), but its transport is inhibited in the presence of the preferred substrate, ammonium (47). The practical advantage of using MA for monitoring Amt activity is the availability of radioactive $^{14}CH_3NH_3^+$ that can be detected by scintillation counting in cell culture uptake experiments (9, 48).

The high specificity for NH_4^+ (and MA) attributed to Amt proteins is noteworthy. Whereas other transport systems, such as aquaporins or potassium channels, are capable of mediating the permeation of ammonium under certain conditions (49, 50), Amt proteins strictly exclude transport of K^+ or H_2O across lipid bilayers (10, 17). To verify and characterize the selectivity of *Af*-Amt1 toward different putative substrates by SSM-based electrophysiology, we applied concentration jumps of MA, dimethylammonium [$(H_3C)_2NH_2^+$; DMA; pK_a = 10.72], Na^+, K^+, and imidazole (pK_a = 7.0) to the same sensor, making the recorded data directly comparable. Under standard conditions (LPR 5:1, pH 7.0), MA and DMA triggered electrogenic responses that reflect a positive charge translocation (Fig. 2) and amounted to 87 ± 8% and 11 ± 4% of the transient currents observed for NH_4^+, respectively. In addition, the peak currents reflect relative transport rates, as seen from the correlation between the magnitude of the peak currents and the respective decay time $\tau_{1/2}$ (*SI Appendix*, Fig. S3 and Table S1). The transport rate for MA was lower than that for ammonium, and the very low transport rate for DMA likely reflects the steric hindrance imposed by the larger cargo molecule. For K^+ and Na^+, no significant differences were detected between the currents obtained with empty vesicles (background) and with reconstituted *Af*-Amt1, supporting the observation that these monovalent cations are not transported (Fig. 2). Moreover, both ions did not seem to interact with the protein, because the same NH_4^+-induced currents were recorded in K^+- or Na^+-free buffers. Contrary to this finding, imidazole and DMA inhibit protein-mediated NH_4^+ transport (Fig. 3), in line with observations on *E. coli* AmtB variants that revealed imidazole bound to the NH_4^+ recruitment site when the protein was crystallized from an imidazole-containing buffer (30, 39).

***Af*-Amt1 NH_4^+ Transport Is pH-Dependent.** For 300 mM ammonium concentration jumps, empty vesicles showed only minor background currents from neutral to acidic pH values (*SI Appendix*, Fig. S2). Up to a pH of 7, >99% of the cargo is in the protonated, cationic form, and judging from the reversibility of the data, the reconstituted protein was stable under all pH conditions tested. Nevertheless, Amt-mediated transport assays at pH > 7.0 generated high background currents that interfered with and ultimately prevented recordings. This result was due to the increasing proportion of membrane-permeable NH_3 and its consequent interaction with lipids from both the sensor and the vesicles. Such effects became apparent at pH 7.5, at [NH_3] ~5 mM, and the system collapsed around [NH_3] of 30 mM. To measure transient currents at pH ≥ 7.5, the total [NH_4^+ + NH_3] was therefore lowered to 30 mM (*SI Appendix*, Fig. S2*A*).

Complete pH titration series from pH 4.0–7.0 and from pH 7.0–9.0 were carried out on the same sensor for direct comparison (Fig. 4). All measurements were started at neutral pH, and

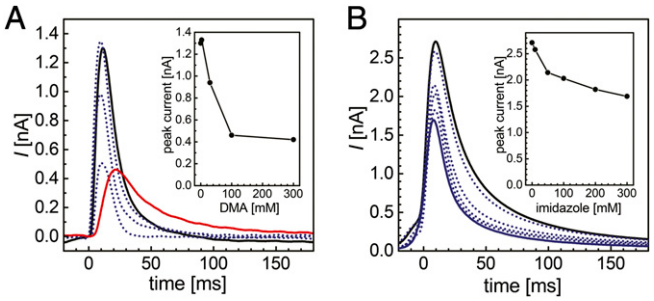

Fig. 3. Inhibition of currents through *Af*-Amt1. (*A*) DMA reduces an initial current response (black). Increasing concentrations of 3, 30, and 100 mM DMA in a background of 300 mM NH_4^+ yield a quick decrease of the effective peak current down to 30% of the initial value (dotted). A concentration of 300 mM DMA without added NH_4^+ (red) leads to a low base current as observed previously (Fig. 2*A*), indicating that DMA is a competitive inhibitor of ammonium transport that itself is not transported efficiently. *Inset* shows the observed peak current variations. (*B*) In a background of 300 mM NH_4^+ at pH 7.0, the addition of imidazole leads to a comparable reduction of peak currents, but a markedly weaker inhibition than the one by DMA. Peak currents are reduced to 70% (*Inset*) at a NH_4^+:imidazole ratio of 1:1 (blue).

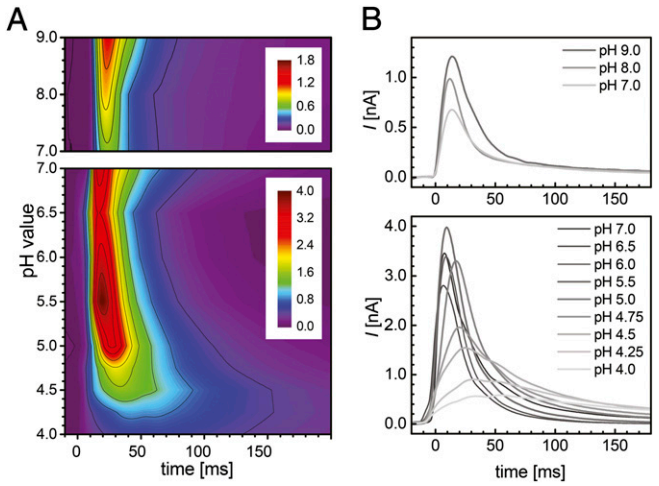

Fig. 4. pH dependence of *Af*-Amt1 transport. Contour plots (*A*) and transient currents (*B*) for different pH values are shown. Starting from pH 7.0, the higher (*Upper*) and lower (*Lower*) pH ranges were studied in separate experiments by using different buffer systems with 30 or 300 mM NH_4^+, respectively (*SI Appendix*, Fig. S2*A*). Maximum currents were observed between pH 5.5 and 6.0. The color scale in *A* is given in [nA].

reversibility was verified throughout. Immobilized vesicles were preequilibrated for at least 30 min per pH unit change (41) with nonactive—i.e., ammonium-depleted solutions. Consequently, these Amt1-mediated NH_4^+ transient currents represent distinct pH equilibrium situations between the luminal and extravesicular solutions rather than different pH (or H^+ gradients) across the vesicle membrane. Under these conditions, the electrogenic activity of *Af*-Amt1 showed a marked pH dependence (Fig. 4); Two regimes were identified: (*i*) a stable plateau from pH 9.0 to 5.5 (*SI Appendix*, Fig. S2*B*); and (*ii*) a strong pH-dependent decrease in the electrogenic response below pH 5.5, such that at pH 4.0 we recorded on average fivefold lower peak currents, concomitant with a fivefold increase in the decay times (Fig. 4). In agreement with our observations at pH 7.0, lower protein densities (LPR of 10:1, 50:1) also led to prolonged decay times at all pH values (*SI Appendix*, Fig. S3).

To determine the kinetics of transport, the peak current intensities of the transients were monitored as a function of NH_4^+ concentration at fixed pH values (Fig. 5). After normalization, the data points for all experiments were best fit by using a Hill equation with $n = 0.6$, suggesting a possible negative cooperativity in NH_4^+ transport. Under these conditions, the apparent half-saturating concentration ($K^{app}{}_{0.5}$) decreased with increasing pH (Fig. 5 and *SI Appendix*, Table S2).

Electrogenic Response of *Af*-Amt2 and *Af*-Amt3. Besides *Af*-Amt1, *A. fulgidus* contains two paralogs, *Af*-Amt2 and *Af*-Amt3. Whereas Amt1 and Amt3 share 64.2% sequence identity, Amt2 is the most dissimilar, with only 39.7% identity toward Amt1 and 40.6% toward Amt3 (24). All proteins contain the common set of conserved and presumably functionally relevant residues (Fig. 1*C*) (1, 6). None of the three proteins was responsive in PLB electrophysiology, but following the analysis of *Af*-Amt1, we initiated SSM-based studies on the other two transporters. The three transporters were purified and reconstituted under identical conditions (*SI Appendix*, *SI Materials and Methods*). Variable protein densities were observed for *Af*-Amt3 (*SI Appendix*, Fig. S4 and Table S3), but the reconstitution efficiency was lower with *Af*-Amt2, and consequently no currents above background levels were obtained to date. In contrast, *Af*-Amt3 consistently triggered electrogenic responses in SSM experiments. Under our standard conditions (LPR 5:1, pH 7.0, 300 mM NH_4^+) the electrogenic response of Amt3 was comparable with that of Amt1 (Fig. 6*A*), with similar rapid current increase and identical average peak currents and decay times. Transient currents obtained with MA (Fig. 6*B*) amounted to <70% of the observed NH_4^+ peak transients, but had comparable decay times that varied with LPR. Together, the data confirm the capacity of Amt3 to transport NH_4^+ in a similar manner to Amt1, in particular if the reconstituted protein densities are normalized (*SI Appendix*, Table S3). Na^+, K^+, and DMA were not transported by *Af*-Amt3 under the applied experimented conditions.

Discussion

Using SSM-based electrophysiology, we present the direct observation of electrogenic ammonium transport by Amt proteins, in a highly defined in vitro system that allows for the assessment of transport rates and substrate specificities. Several considerations lead us to the conclusion that the measured currents correspond to the specific electrogenic activity of *Af*-Amt1 and *Af*-Amt3. First, the transient currents measured were 10-fold higher than the background. Second, the transients have decay times that vary with the LPR—the higher the protein density, the faster the decay time, indicating that the currents reflect the charging of the vesicles due to an electrogenic transport of substrate (46, 51). Third, our recordings corroborate the expected selectivity sequence for Amt, with ammonium being the substrate with the highest transport rate, followed by MA and DMA. Sodium and potassium were not found to interact with the proteins. Fourth, the pH titrations from pH 7 to 4 show a correlation between the magnitude of the peak currents and the decay times, whereas the background recordings at those pH values present identical amplitudes and decay times. The data thus unequivocally show the electrogenic nature of *Af*-Amt1 transport.

Taking into account the turnover values reported for two secondary active transporters, LacY and the *E. coli* chloride/proton antiporter (*Ec*-ClC), and the magnitude of the observed signals in both cases, it was concluded that 10^8 to 10^9 transporters can be simultaneously investigated with the SSM technique (41, 46). Because the particle densities obtained with trimeric *Af*-Amt1 and *Af*-Amt3 at LPR 5 lie in between the particle densities observed with monomeric LacY at LPR 5 (4,500 particles per μm^2) and dimeric *Ec*-ClC at LPR 25 (75 particles per μm^2), the above estimate should hold true for the Amt proteins investigated here. Thus, from its average current amplitude (2.2 nA), the turnover of *Af*-Amt1 should be in the

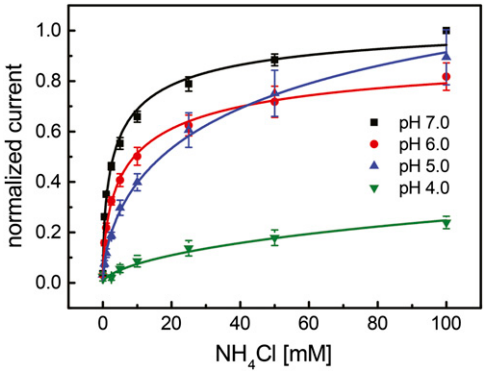

Fig. 5. Substrate dependence of NH_4^+ currents in *Af*-Amt1 at different pH values. In every case, the currents show saturation behavior, as expected for a protein-mediated transport process, with half-maximal values increasing with pH. Best fits were obtained after normalization, with a Hill equation using $n = 0.6$ (*SI Appendix*, Table S2).

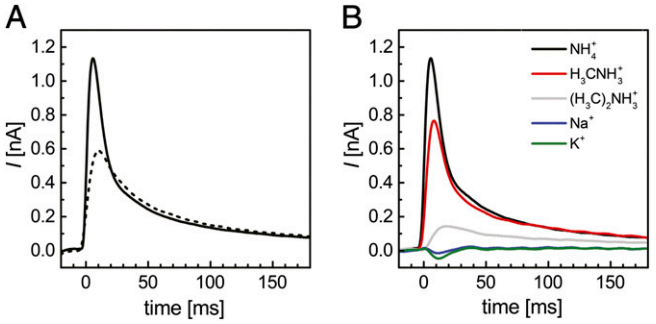

Fig. 6. Electrogenic responses of *Af*-Amt3. (*A*) At LPR of 5:1 (solid) and 10:1 (dashed), the orthologous Amt3 shows a response that is very similar to the one of Amt1 (Fig. 1*B*). Note the increase of decay time at the higher LPR (15 ± 3 and 38 ± 2, respectively). (*B*) Amt-3 shows a substrate dependence that corresponds to the one of Amt-1 (Fig. 2*A*), with strong currents observed for NH_4^+ and MA, only weak conductance of DMA, and impermeability for Na^+ and K^+.

range of 30–300 NH_4^+ ions per s per trimer. This result is in the range of other transporters, such as LacY (46), but far below the conductances observed in ion channels. *Af*-Amt1 exhibited the highest apparent affinity for ammonium, $K_{0.5}$ = 1–8 mM with a Hill coefficient of $n = 0.6$ between pH 6.0 and 8.0, with a significant decrease outside of this pH range. Published half-saturating concentrations for Amt family members are in the micromolar range (2–50 μM) (11, 52). However, these affinities were determined in voltage-clamp experiments using reconstituted protein in oocytes, where a transmembrane voltage is imposed, and they were reported to depend on the holding potential (10, 52, 53). There are no holding potentials in an SSM experiment, and if the published voltage-clamp data are fit with a Boltzmann equation to extrapolate the voltage-dependent $K_{0.5}$ values to zero potential, they approach the millimolar range, in line with our data.

We could confirm the high selectivity of Amt proteins for NH_4^+ and MA, and we showed that both K^+ and Na^+ ions do not interact with the protein. This finding was not the case for DMA or imidazolium, because their presence decreased NH_4^+ currents through Amt-1 significantly. Whereas DMA itself was transported at a low rate, imidazolium only bound to the protein, acting as a competitive inhibitor of ammonium transport. We were able to address the effect of pH on affinities and transport rates of ammonium under equilibrium conditions. From the observed changes, we conclude that the protein sensed and responded to environmental pH, such that the transient current peaks for ammonium remained constant between 8.0 ≥ pH ≥ 5.5, but dropped by 80% from pH 5.5 to 4.0. All signals were reversible for the entire pH range tested. The major effect of environmental pH on the transport kinetics of *Af*-Amt1 occurred through changes in substrate affinity rather than in the overall transport rates (Fig. 5 and *SI Appendix*, Table S2). Data at higher pH values were harder to obtain, as the experimental conditions approached the pK_a value of the NH_3/NH_4^+ pair. Interestingly, a fit of the observed kinetic profiles with a Hill equation consistently refined to a Hill coefficient of $n = 0.6$. A Hill coefficient below unity indicates negative cooperativity, and this result is in line with previous data that showed deletions or mutations in the C terminus region to severely hinder transport (33, 53, 54). The structure of *Af*-Amt1 revealed that the C terminus is in close contact with the neighboring monomer, and a subsequent study provided evidence for a phosphorylation-based feedback regulation mediated by the C terminus of *Arabidopsis thaliana* AMT1;1 (55). The C termini of the Amt protomers thus are well positioned to coordinate structural changes that might form the basis for the observed cooperative action in transport.

In conclusion, the higher sensitivity of the SSM method was essential, because Amt proteins are slow transporters that do not generate sufficiently large currents for measurements on the far smaller membrane area of a planar lipid bilayer experiment. Under controlled in vitro conditions, we detected substrate-dependent currents for Amt1 and Amt3, confirming both proteins to be electrogenic ammonium transporters. The stability of a typical sensor allowed us to study systematic variations of substrate concentration and pH and assured us that the experiments are reversible.

Experimental Procedures

SSM Electrophysiology. A solution of 10 mM octadecanethiole (Sigma-Aldrich) in ethanol (pro analysis) was incubated overnight with a gold electrode assembly. The electrode was then incubated for 30 min with 2 μL of a mixture containing 16.5 mg·mL^{-1} diphytanoyl phosphatidylcholine (Avanti) and 0.28 mg·mL^{-1} octadecylamine (Alfa Aeser) in *n*-decane. The resulting hybrid bilayer of phosphatidylcholine:octadecanethiol linked to the gold electrode surface formed the SSM sensor element and functioned as the measuring electrode (40). This sensor was mounted into a flow-through cuvette, preserving an inner reaction volume of 17 μL, and the circuit was connected to an Ag/AgCl reference electrode (56). The formation and quality of the SSM was controlled by its capacitance and conductance characteristics. Typical values ranged between 0.3 and 0.5 μF·cm^{-2} for the capacitance and 0.05 and 1.0 μS·cm^{-2} for the conductance.

A detailed description of the protocols used for protein purification and reconstitution into proteoliposomes is provided in *SI Appendix, SI Materials and Methods*. A total of 40 μL of a proteoliposome suspension containing 2 mg·mL^{-1} protein (in vesicles prepared at 5:1 LPR) was loaded into the cuvette and allowed to adsorb onto the sensor element for 60–70 min. All experiments were carried out with a working pressure of 0.6 bar, and the ambient temperature was kept between 20 and 23 °C. Protein-mediated transport events were triggered by rapid solution exchange driven by two-way isolation valves (NResearch). Typically, the system was sequentially flushed with nonactive solution by using two cycles of 2.5-s step duration and a single 2.0-s step with active solution in between. All low-pH solutions, with 4.0 ≤ pH ≤ 7.5, were prepared in 100 mM KP_i and 25 mM tripotassium citrate buffer. We used 100 mM Tris/HCl in the range of 8.0 ≤ pH ≤ 8.5 and 100 mM glycine/KOH for pH ≥ 9.0. To suppress background current artifacts, 500 mM KCl was added to the solutions. In addition, the active solution contained variable amounts (*x* mM) NH_4Cl and 300-*x* mM NaCl, whereas the inactive solution invariably contained 300 mM NaCl. Experiments conducted at various pH values were performed on the same membrane after incubating the system in the new nonactive solution for 30 min (41).

To investigate the relationship between peak currents and the ammonium concentration, each equivalent of NH_4Cl added or taken from the active solutions was balanced with KCl for constant overall osmolality.

Transient currents were amplified with a current amplifier (Keithley; model 428). The gain was set to 10^9 V/A with a low-pass filtering in the range of 100 Hz.

Statistical Analysis. Various protein batches and thus reconstituted protein samples were tested. All measurements were recorded at least in triplicate and using three different sensors. For the transport kinetics, the peak currents were normalized to the currents measured by using 100 mM ammonium concentration jumps at pH 7.0 in experiments carried out from pH 4.0–7.0 and to 30 mM ammonium concentration jumps at pH 7.0 in experiments conducted at pH ≥ 7.5.

ACKNOWLEDGMENTS. We acknowledge the assistance and support of the Center for Microscopy and Image Analysis, University of Zürich, for the freeze-fracture and transmission electron microscopy experiments. This work was supported by Deutsche Forschungsgemeinschaft Grants AN 676/1 and AN 676/3 (to S.L.A.A.).

1. Andrade SL, Einsle O (2007) The Amt/Mep/Rh family of ammonium transport proteins. *Mol Membr Biol* 24(5-6):357–365.
2. Javelle A, et al. (2007) Structural and mechanistic aspects of Amt/Rh proteins. *J Struct Biol* 158(3):472–481.
3. Ludewig U, Neuhäuser B, Dynowski M (2007) Molecular mechanisms of ammonium transport and accumulation in plants. *FEBS Lett* 581(12):2301–2308.
4. Tremblay PL, Hallenbeck PC (2009) Of blood, brains and bacteria, the Amt/Rh transporter family: Emerging role of Amt as a unique microbial sensor. *Mol Microbiol* 71(1):12–22.

5. Nakhoul NL, Hamm LL (2004) Non-erythroid Rh glycoproteins: A putative new family of mammalian ammonium transporters. *Pflugers Arch* 447(5):807–812.
6. Winkler FK (2006) Amt/MEP/Rh proteins conduct ammonia. *Pflugers Arch* 451(6): 701–707.
7. Kleiner D (1981) The transport of NH_3 and NH_4^+ across biological membranes. *Biochim Biophys Acta* 639(1):41–52.
8. Kleiner D, Fitzke E (1981) Some properties of a new electrogenic transport system: The ammonium (methylammonium) carrier from *Clostridium pasteurianum*. *Biochim Biophys Acta* 641(1):138–147.
9. Stevenson R, Silver S (1977) Methylammonium uptake by *Escherichia coli*: Evidence for a bacterial NH_4^+ transport system. *Biochem Biophys Res Commun* 75(4):1133–1139.
10. Ludewig U, von Wirén N, Frommer WB (2002) Uniport of NH_4^+ by the root hair plasma membrane ammonium transporter LeAMT1;1. *J Biol Chem* 277(16):13548–13555.
11. Mayer M, Dynowski M, Ludewig U (2006) Ammonium ion transport by the AMT/Rh homologue LeAMT1;1. *Biochem J* 396(3):431–437.
12. Mayer M, Ludewig U (2006) Role of AMT1;1 in NH_4^+ acquisition in *Arabidopsis thaliana*. *Plant Biol (Stuttg)* 8(4):522–528.
13. Nakhoul NL, et al. (2005) Characteristics of renal Rhbg as an $NH_{4(}^+$) transporter. *Am J Physiol Renal Physiol* 288(1):F170–F181.
14. Westhoff CM, Ferreri-Jacobia M, Mak DO, Foskett JK (2002) Identification of the erythrocyte Rh blood group glycoprotein as a mammalian ammonium transporter. *J Biol Chem* 277(15):12499–12502.
15. Ludewig U (2004) Electroneutral ammonium transport by basolateral rhesus B glycoprotein. *J Physiol* 559(Pt 3):751–759.
16. Soupene E, He L, Yan D, Kustu S (1998) Ammonia acquisition in enteric bacteria: Physiological role of the ammonium/methylammonium transport B (AmtB) protein. *Proc Natl Acad Sci USA* 95(12):7030–7034.
17. Khademi S, et al. (2004) Mechanism of ammonia transport by Amt/MEP/Rh: Structure of AmtB at 1.35 A. *Science* 305(5690):1587–1594.
18. Lande MB, Donovan JM, Zeidel ML (1995) The relationship between membrane fluidity and permeabilities to water, solutes, ammonia, and protons. *J Gen Physiol* 106(1):67–84.
19. Boogerd FC, et al. (2011) AmtB-mediated NH_3 transport in prokaryotes must be active and as a consequence regulation of transport by GlnK is mandatory to limit futile cycling of $NH_{4(}^+$)/NH_3. *FEBS Lett* 585(1):23–28.
20. Arcondéguy T, Jack R, Merrick M (2001) $P_{(II)}$ signal transduction proteins, pivotal players in microbial nitrogen control. *Microbiol Mol Biol Rev* 65(1):80–105.
21. Zheng L, Kostrewa D, Bernèche S, Winkler FK, Li XD (2004) The mechanism of ammonia transport based on the crystal structure of AmtB of *Escherichia coli*. *Proc Natl Acad Sci USA* 101(49):17090–17095.
22. Gruswitz F, O'Connell J, 3rd, Stroud RM (2007) Inhibitory complex of the transmembrane ammonia channel, AmtB, and the cytosolic regulatory protein, GlnK, at 1.96 A. *Proc Natl Acad Sci USA* 104(1):42–47.
23. Conroy MJ, et al. (2007) The crystal structure of the *Escherichia coli* AmtB-GlnK complex reveals how GlnK regulates the ammonia channel. *Proc Natl Acad Sci USA* 104(4):1213–1218.
24. Andrade SL, Dickmanns A, Ficner R, Einsle O (2005) Crystal structure of the archaeal ammonium transporter Amt-1 from *Archaeoglobus fulgidus*. *Proc Natl Acad Sci USA* 102(42):14994–14999.
25. Li X, Jayachandran S, Nguyen HH, Chan MK (2007) Structure of the *Nitrosomonas europaea* Rh protein. *Proc Natl Acad Sci USA* 104(49):19279–19284.
26. Lupo D, et al. (2007) The 1.3-A resolution structure of *Nitrosomonas europaea* Rh50 and mechanistic implications for NH_3 transport by Rhesus family proteins. *Proc Natl Acad Sci USA* 104(49):19303–19308.
27. Gruswitz F, et al. (2010) Function of human Rh based on structure of RhCG at 2.1 A. *Proc Natl Acad Sci USA* 107(21):9638–9643.
28. Guan L, Kaback HR (2006) Lessons from lactose permease. *Annu Rev Biophys Biomol Struct* 35:67–91.
29. Monahan BJ, et al. (2002) Mutation and functional analysis of the *Aspergillus nidulans* ammonium permease MeaA and evidence for interaction with itself and MepA. *Fungal Genet Biol* 36(1):35–46.
30. Javelle A, et al. (2006) An unusual twin-his arrangement in the pore of ammonia channels is essential for substrate conductance. *J Biol Chem* 281(51):39492–39498.
31. Marini AM, Boeckstaens M, Benjelloun F, Chérif-Zahar B, André B (2006) Structural involvement in substrate recognition of an essential aspartate residue conserved in Mep/Amt and Rh-type ammonium transporters. *Curr Genet* 49(6):364–374.
32. Fong RN, Kim KS, Yoshihara C, Inwood WB, Kustu S (2007) The W148L substitution in the *Escherichia coli* ammonium channel AmtB increases flux and indicates that the substrate is an ion. *Proc Natl Acad Sci USA* 104(47):18706–18711.
33. Severi E, Javelle A, Merrick M (2007) The conserved carboxy-terminal region of the ammonia channel AmtB plays a critical role in channel function. *Mol Membr Biol* 24(2):161–171.
34. Boeckstaens M, André B, Marini AM (2008) Distinct transport mechanisms in yeast ammonium transport/sensor proteins of the Mep/Amt/Rh family and impact on filamentation. *J Biol Chem* 283(31):21362–21370.
35. Lin Y, Cao Z, Mo Y (2006) Molecular dynamics simulations on the *Escherichia coli* ammonia channel protein AmtB: Mechanism of ammonia/ammonium transport. *J Am Chem Soc* 128(33):10876–10884.
36. Inwood WB, Hall JA, Kim KS, Fong R, Kustu S (2009) Genetic evidence for an essential oscillation of transmembrane-spanning segment 5 in the *Escherichia coli* ammonium channel AmtB. *Genetics* 183(4):1341–1355.
37. Nygaard TP, Alfonso-Prieto M, Peters GH, Jensen MO, Rovira C (2010) Substrate recognition in the Escherichia coli ammonia channel AmtB: A QM/MM investigation. *J Phys Chem B* 114(36):11859–11865.
38. Hall JA, Kustu S (2011) The pivotal twin histidines and aromatic triad of the *Escherichia coli* ammonium channel AmtB can be replaced. *Proc Natl Acad Sci USA* 108(32): 13270–13274.
39. Javelle A, et al. (2008) Substrate binding, deprotonation, and selectivity at the periplasmic entrance of the *Escherichia coli* ammonia channel AmtB. *Proc Natl Acad Sci USA* 105(13):5040–5045.
40. Schulz P, Garcia-Celma JJ, Fendler K (2008) SSM-based electrophysiology. *Methods* 46(2):97–103.
41. Garcia-Celma J, Szydelko A, Dutzler R (2013) Functional characterization of a ClC transporter by solid-supported membrane electrophysiology. *J Gen Physiol* 141(4): 479–491.
42. Seifert K, Fendler K, Bamberg E (1993) Charge transport by ion translocating membrane proteins on solid supported membranes. *Biophys J* 64(2):384–391.
43. Garcia-Celma JJ, Hatahet L, Kunz W, Fendler K (2007) Specific anion and cation binding to lipid membranes investigated on a solid supported membrane. *Langmuir* 23(20):10074–10080.
44. Garcia-Celma JJ, et al. (2008) Rapid activation of the melibiose permease MelB immobilized on a solid-supported membrane. *Langmuir* 24(15):8119–8126.
45. Garcia-Celma JJ, Ploch J, Smirnova I, Kaback HR, Fendler K (2010) Delineating electrogenic reactions during lactose/H^+ symport. *Biochemistry* 49(29):6115–6121.
46. Garcia-Celma JJ, Smirnova IN, Kaback HR, Fendler K (2009) Electrophysiological characterization of LacY. *Proc Natl Acad Sci USA* 106(18):7373–7378.
47. Hackette SL, Skye GE, Burton C, Segel IH (1970) Characterization of an ammonium transport system in filamentous fungi with methylammonium-^{14}C as the substrate. *J Biol Chem* 245(17):4241–4250.
48. Servín-González L, Bastarrachea F (1984) Nitrogen regulation of synthesis of the high affinity methylammonium transport system of *Escherichia coli*. *J Gen Microbiol* 130(12):3071–3077.
49. Holm LM, et al. (2005) NH_3 and NH_4^+ permeability in aquaporin-expressing *Xenopus* oocytes. *Pflugers Arch* 450(6):415–428.
50. Moroni A, Bardella L, Thiel G (1998) The impermeant ion methylammonium blocks K^+ and NH_4^+ currents through KAT1 channel differently: Evidence for ion interaction in channel permeation. *J Membr Biol* 163(1):25–35.
51. Mager T, Rimon A, Padan E, Fendler K (2011) Transport mechanism and pH regulation of the Na+/H+ antiporter NhaA from Escherichia coli: An electrophysiological study. *J Biol Chem* 286(26):23570–23581.
52. Ortiz-Ramirez C, Mora SI, Trejo J, Pantoja O (2011) PvAMT1;1, a highly selective ammonium transporter that functions as H^+/$NH_{4(}^+$) symporter. *J Biol Chem* 286(36): 31113–31122.
53. Neuhäuser B, Dynowski M, Mayer M, Ludewig U (2007) Regulation of NH_4^+ transport by essential cross talk between AMT monomers through the carboxyl tails. *Plant Physiol* 143(4):1651–1659.
54. Marini AM, Springael JY, Frommer WB, André B (2000) Cross-talk between ammonium transporters in yeast and interference by the soybean SAT1 protein. *Mol Microbiol* 35(2):378–385.
55. Loqué D, Lalonde S, Looger LL, von Wirén N, Frommer WB (2007) A cytosolic transactivation domain essential for ammonium uptake. *Nature* 446(7132):195–198.
56. Zhou A, et al. (2004) Charge translocation during cosubstrate binding in the Na^+ /proline transporter of *E. coli*. *J Mol Biol* 343(4):931–942.